In situ experimental and theoretical studies of the performance and the fouling impact of shower grey water heat recovery systems

Jean-Baptiste Bouvenot, Cyprien Beaudet

Energy & Buildings 331 (2025) 115341

Contents lists available at ScienceDirect

Energy & Buildings

journal homepage: www.elsevier.com/locate/enb

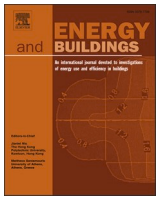

In situ experimental and theoretical studies of the performance and the fouling impact of shower greywater heat recovery systems

Jean-Baptiste Bouvenot [a,b,*], Cyprien Beaudet [a]

[a] ICube Laboratory University of Strasbourg France
[b] INSA Strasbourg, 24 Boulevard de la Victoire 67000 STRASBOURG, France

ARTICLE INFO

Keywords:
Grey water
Drain water
Shower
Heat recovery
Heat exchanger
Fouling
Domestic Hot Water

ABSTRACT

This paper begins with a theoretical analysis of shower water heat recovery systems, assessing 3 key indicators in particular: the V40 indicator (volume of water that can be produced at 40 °C), the efficiency of the heat exchanger and the efficiency of the complete system. A benchmark was also carried out on commercial systems available, with a classification by type. Finally, a comparative and critical analysis was carried out on tests standards. Next, a model of fouling by biofilm development is proposed, then validated and calibrated experimentally. Then, this work presents the results of a in situ gravity grey-shower-drain water heat recovery system (plates) test campaign over 14 months and a theoretical analysis of this type of system, studying the different types of connections and the impact of influencing parameters (flow rate, temperature, user profile). This work provides experimental data on actual performance and characterizes fouling of this type of exchanger through biofilm development and show the good performance of these systems that can provide a significant impact on the whole energy balance of buildings. The average efficiency of the recovery heat exchanger, taking fouling into account, is 66 %, i.e. 8 % less than the nominal efficiency. Finally, the efficiency of the overall system was evaluated at 52 %, which means that DHW consumption in a dwelling can be drastically reduced with this type a low-tech system. This study also shows the significant impact of the fouling on the performance that requires to treat this question to ensure a sustainable operation over time.

1. Introduction

Domestic hot water (DHW) is a major source of energy consumption in residential buildings (the second behind heating), accounting for 16 % [1,2] in France in 2021 (15 % in Europe in 2021 [3], 18 % in the United States in 2011 [4]). This rate has grown steadily, doubling over the past 50 years in France [1,2] as a result of improvements in building thermal performance (increasingly stringent buildings thermal regulations) and a higher level of comfort, notably with more frequent showers. The energy consumed for DHW devoted to showers in France represents around 49 TWh in 2021 [1], of which 24 TWh [1] is produced with electrical energy, mainly with Joule-effect electrical heaters (between 10 and 15 M of units) that mainly operate at night during off-peak hours. This base power load is mainly covered by nuclear power plants in France. This represents the output power production of around 2 nuclear reactors (over 57 in France in 2024). Among DHW consumption, shower-related consumption accounts for around 2/3 of the total. It turns out that this is also the easiest source of heat to recover ("lightly charged" grey water (i.e. oily water)) compared with "heavily charged" grey water from dishwashing. In addition to the gains in energy efficiency and GHG emissions, recovering some of this energy is also an opportunity to release power capacities regarding the growing use of electric mobility, which will require large quantities of energy during this same night-time period when vehicles recharge their batteries. Mostly, one work to improve DHW production (thermodynamic hot water tanks, heat pumps, thermal solar panels, biomass, etc.) without bothering to recover the waste heat from the evacuation of still-warm grey water. Yet this is what is done with a double-flow ventilation system, for example. In terms of energy quality, by considering an ambient environment at $T_0 = 273K$ and a drain temperature at $T_{drain} = 307K(34^{\circ}C)($ (from our own measurements and on literature review [5–7]), a shower uses a low part (30 %) of the incident exergy Ex_{tot} contained in DHW at 40 °C (see Fig. 1). Besides, in terms of energy quantity, the result is worst with only 20 % of the total heat produced which is used in the most favourable case (cold water T_{cw} from the district networks at 10 °C heat up to hot water drawn off T_{dhw} at 40 °C and drain water T_{drain} at 34 °C) that corresponds to the heat which is

* Corresponding author at: ICube Laboratory, University of Strasbourg, France.
E-mail address: jean-baptiste.bouvenot@insa-strasbourg.fr (J.-B. Bouvenot).

https://doi.org/10.1016/j.enbuild.2025.115341
Received 30 September 2024; Received in revised form 20 December 2024; Accepted 16 January 2025
Available online 27 January 2025

Nomenclature

C_{dyn}	dynamic coefficient,- or %
c_p	water specific heat capacity, J.kg^{-1}.K^{-1}
E	heat exchanger efficiency, % or –
E	energy, J or kWh
Ex	exergy, J
$\dot{E}x$	exergy flux, W
GHG	Green House Gas,
k_f	fouling coefficient, kW.K^{-1}.m^{-2}.d^{-2}
NTU	Number of Transfer Units, –
$\dot{Q}$	thermal power, W
q_v	water volume-flow rate, m^3.s^{-1}
R	flow unbalance factor,-
R	thermal resistance m^2.K.W^{-1}
S	exchange surface, m^2
T	duration, s
T	temperature, K or °C
t	time, s or min or day
US	thermal conductance, W.K^{-1}
V	volume of the tank, l
$\dot{V}$	volume flow rate, l.min^{-1}
$V40$	volume of DHW at 40 °C drawn off

Greek symbols

ϕ	heat flux, W
ρ	water density, kg.m^{-3}
υ_{40}	relative gain on V_{40}, –

Indexes and exponents

0	reference
∞	asymptotic value
c	cold
cw	district cold water
dhw	domestic hot water
drain	drain water/grey water
exp	experimental
f	fouling
FE	final energy
gr	growth
hw	hot water
HX	Heat eXchanger
I	inflexion
i	inlet
ind	induction
min	minimum
mix	mixed water at 40 °C
o	outlet
PE	primary energy
ph	preheated
rec	recovered
ss	steady state
syst	system
tank	DHW tank
th	theoretical
tot	total
used	used

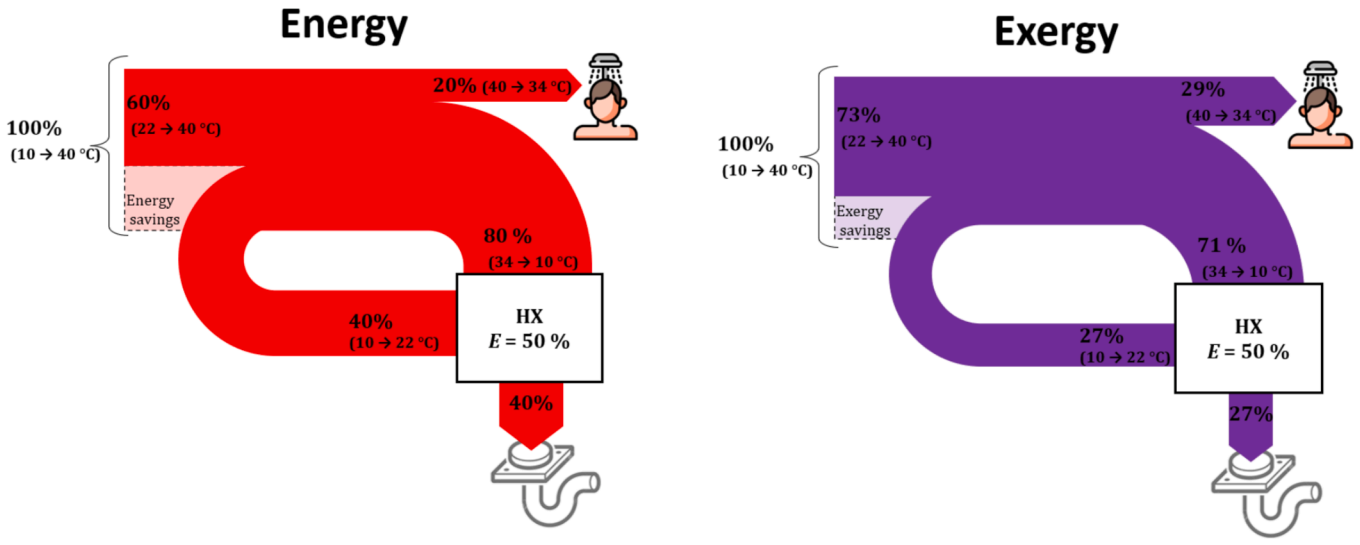

Fig. 1. Sankey diagram showing the potential energy and exergy gains provided by a grey water heat recovery unit (the efficiency has been arbitrarily set at 50%: average of values for commercial systems).

used/lost between the shower head and the drain (see Fig. 1). 80 % of the heat produced will be evacuated via the drainage system as waste heat. This rate is also mentioned by Cooperman et al [8] (10 to 20 %), who also mention a total waste heat quantity of 350 TWh/year for the United States. So it makes sense to try to harvest this large quantity of heat, which is usually considered as a waste product. It is relatively easy to recover it, either via passive, gravity-driven heat exchangers (see Fig. 1), or via active, thermodynamic systems that use this waste heat as a cold source. Some authors like Hervás-Blasco et al [5] studied the use of a heat pump to valorise this waste heat but the advantages of the first solution are its low-tech nature, low maintenance (no moving parts), long lifetime and low cost. The major disadvantage lies in its integration, since it involves a gravity heat exchanger that ideally needs to be below and as close as possible to the shower drain, which is not always possible (full floor house or flats).

The characteristics of grey water heat recovery exchangers are special because of the gravity flow and potentially free surface, requiring low pressure drops, and because of the 'charged' fluids (slightly oily grey water), which generate fouling. Many authors worked on drain water heat recovery systems. Some authors worked on their own prototypes

[6,7,9–12], but the majority of the studies deals with commercial systems by studying them experimentally [13–21], numerically or theoretically [5,22,23] of both too [24,25]. Experimental tests are mainly laboratory tests and to our knowledge, no author has published detailed experimental results from in situ tests as it's proposed here. About theoretical studies, the widespread Number of Transfer Units (NTU) and the logarithmic mean temperature difference (LMTD) methods are almost systematically used [11–13,19]. Beentjes et al [15] specifically studies the impact of the angle of inclination of falling film heat exchangers in the steady regime but this only concerns vertical falling film exchangers. Manouchehri et al [17] works mainly on the impact of water temperatures on system efficiency and demonstrates a significant impact. Manouchehri et al [18] also shows the impact of the flow rate, which does not necessarily follow the NUT theory (impact of flow speeds on the exchange coefficient), which will also be shown here. Plate heat exchangers are also little studied [7,12] even though they are among the most efficient, which is precisely the subject of study in this publication. But only a few authors try to take into account unsteady effects [6,10,20–23,25] or the effect of the variation of the flow parameters (temperature and/or mass flow rate) on the HX exchange coefficient [9,13,15–19,24]. A few authors propose taking inertial effects into account [22,23,25,26,6], but these are essentially limited to first-order models with no delay time. Selimli et al [6] proposes an original approach with Blotzmann curve fitting. The present study proposes to take better account of these dynamic effects (delay time, impact of the sequence of showers). Finally, although some authors refer to the importance of considering the HX fouling (biofilm development, hair, sand, grease, dead skin…) [6,26,27], but none propose a specific work on this question, especially for long-term in situ tests. Only Grunden et al [26], Wänner [27] and Shen et al [28–30] worked specifically on this topic. Grunden et al [26] carried out in-situ tests on an experimental prototype, but was unable to really characterize the fouling with a protocol that proved unsuitable. Wanner [27] grew biofilm on plates in laboratory conditions and was able to measure the impact on plates thermal conductance. He was also able to assess the performance of rinsing/cleaning (or purging), showing a loss limitation of around 20 % (50 % loss without rinsing).Shen et al [28–30] propose an in-depth study (but only over a few weeks) on the fouling of a serpentine heat exchanger immersed in a grey water recovery tank to boost the performance of a heat pump for DHW production. The state of the art has already demonstrated the relevance of this type of robust, reliable and long-lasting system and its good performance, particularly for vertical coaxial systems [12] or plate heat exchangers [18] with exchanger efficiencies of up to 60 to 80 %. However, these results are essentially based on laboratory tests, under steady state conditions, without taking into account dynamic or fouling effects. The majority of the tests did not use real grey water, simulating a shower only via the temperature at which it is drawn off and its flow rate. Most of these studies simply optimize the design of certain types of exchanger, or compare their experimental results with the NUT theory, but none of them offers extensive feedback involving use under real conditions (variable flow rates and drain water temperatures, variable profiles, fouling, exchanger inertia).

There are several novelties from this work. At first, this publication provides an original theoretical analysis involving the calculation of 3 performance indicators (exchanger efficiency, exchanger efficiency and V40: volume of water that can be produced at 40 °C) according to several parameters (hydraulic connexions, volume flow rate, user profiles). In particular, the study on V40 indicator has been seen in the literature. Then, this work provides a detailed analysis (6 s time step) of in situ data over a period of 14 months. Besides, this work provides a detailed analysis of experimental data to characterise dynamic phenomena (inertia, delay time, sequence of draw-offs) and fouling. Finally, this work provides development of a data-driven model for dynamic effects and fouling. This study is one of the few to quantify the overall performance of a complete system (DHW tank + heat recovery units) under real conditions over a full year. This work proposes an original theoretical and experimental approach to better understand the performance of this type of system under real-life conditions, taking into account various phenomena in a combined manner: unsteady effects, fouling due to biofilm development, hydraulic connections, and user profile. This work proposes an analysis on gravity shower grey water heat recovery systems only based on in situ tests and heat exchangers theory.

Table 1
Drain water heat recovery exchanger test standards.

	KIWA [31]	**CSTB** [32]	**CSA** [33]	**In Situ test**
T_{drain}	40 °C	37 °C	40 °C	34 °C (36 °C for children and 33 °C for adults)
T_{cwi}	10 °C	12,8°C	12 °C	from 10 to 20 °C (mean at 15 °C)
T_{mix}	–	40 °C	–	40 °C
T_{tank}	–	55 °C	–	55 °C
q_v	5,8–9,2 and 12,5 l.min^{-1}	8 l. min^{-1}	9,5 l. min^{-1}	4,2 l.min^{-1} (mean value)
Balanced case	yes	yes	yes	yes
Unbalanced case	no	yes	no	no
Transient effects	no	yes	no	yes
Fouling effects	no	no	no	yes

2. State of the art of drain water recovery heat exchanger

2.1. State of the art of testing standards

Performance tests for drain water heat recovery units are governed by various international standards. There are 4 main standards from different certification institutes: KIWA from the Netherlands [31], CSTB-RECADO protocol from France [32], CSA from Canada [33] and IAPMO from USA [34] which is based on the Canadian standard. These standards differ in that they consider different test protocols. Only the French standard specifies for example an indicator relating to the heat exchanger's thermal inertia (transient coefficient) that considers the heat exchanger's temperature rise. No standard considers the effects of fouling. Table 1 summarizes the test conditions for each standard compared to in situ results.

2.2. Hydraulic connections configurations and hypothesis

We propose here a theoretical approach to compute the thermal performance of a drain water heat recovery exchanger DWHRX. At first we have to present the 3 main configurations in terms of hydraulic connections we can find for this kind of systems (see Fig. 2) and which are described in the French standard [32] or by others authors [35–37]:

It can be noted that for the configuration where DHW production is instantaneous (without storage tank), even if the connection is only to the mixing valve (configuration 2), from a calculation point of view, performance corresponds to configuration 1, since all the flow transits through the HX. The following assumptions are made (the values in bold are the reference values):

– total DHW mass flow rate (shower head to drain): q_v = [4;6;**8**;10;12] l.min^{-1}.

– cold water mass flow rate supplying the mixing valve to mitigate the hot tank water: q_{v_cw} (variable according to configuration, see Fig. 2).

– cold water mass flow rate supplying the DHW tank (=mass flow rate of hot water from the tank connected to the mixing valve): q_{v_tank} (variable according to configuration see Fig. 2).

– district cold water: T_{cwi} = **12.8**°C (normative value from French

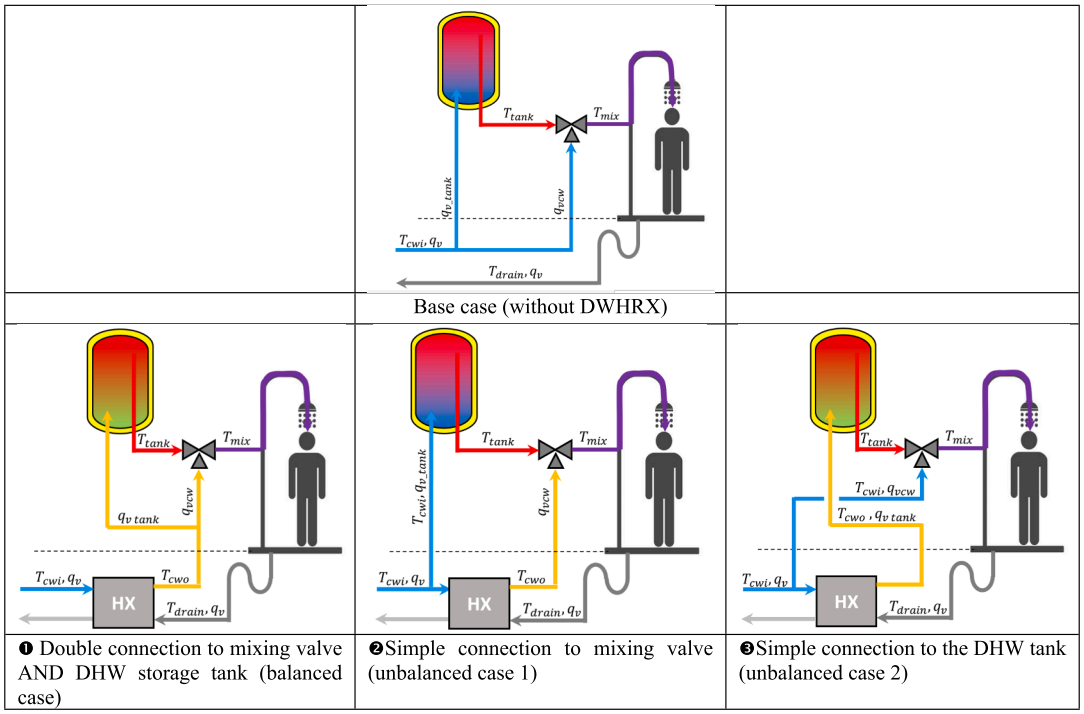

Fig. 2. Schematic diagrams of the 3 hydraulic connection configurations.

Table 2
DWHRX market survey.

HX type	Technology	Manufacturer	Reference	Nominal efficiency	Certifications / Tests conditions	Cost [€]	Specific cost [€/kW]	Maintenance
Horizontal	Integrated in the shower tray	Evolsys	Evoslim	37,0%	KIWA [31] T_{drain} = 35 °C	1 000 €	200	Limited manual maintenance with detergent
		Recoup	Recoup Tray + DSS-S2	45,8%	–	1 000 €	162	Easily accessible system, manual drain with brush and detergen
	Integrated into the shower drain	Evolsys	ShowerDrain	34,0%	RECADO [32] KIWA [31]	1 400 €	305	
		Wagner Solar	ECOshower 900	49,1%	–	–		
		Recoup	Recoup Drain +	49,1%	–	1 400 €	211	
		Gaïa Green	ReQup-Floor	43,0%	RECADO [32]	1 360 €	234	
		Joulia	Joulia Drain Water 5P-630-F	39,0%	KIWA [31]	1 976 €	376	
	Installed under the baththub	Evolsys	Evobox	43,0%	KIWA [31] RECADO [32]	1 000 €	172	System manually inaccessible, purge with detergent only
		Recoup	Recoup EASYFIT +	46,4%		1 000 €	160	
	Installed under the shower / along the drain pipe	Reccal	Turbosiphon	18,0%	RECADO [32]	359 €	148	
		EHTech	***Obox****	***71,0%***	***RECADO*** [32]	***800 €***	***83***	***System manually inaccessible, automatic purge***
		WiseElement	Ekô	40 %*	*in the process of certification	800 €	148	System manually inaccessible, purge with detergent only
		EcoDrain	Eco-Drain	–	–	–		
		Zypho	IZI 40	33,0%	KIWA [31]	820 €	185	
			SLIM 50	49,0%	RECADO [32]	Not yet available	–	
Vertical		Norellagg	Shower Pipe R 50–300	64,6%	RECADO [32]	1 100 €	126	
		Thermo Drain	TDH3620B	57,2%	CSA [33]	900 €	117	
		Renew abilty	Power Pire R4-96	68,0%	CSA [33]	1 323 €	144	
		Zypho	ZYYPI75S2200	69,2%		780 €	84	
		Gaïa Green	Showersave QB1-21	66,0%	KIWA [31] RECADO [32]	847 €	95	
		Recoup	Recoup PIPE + HE	63,7%	–	1 000 €	116	
		Evolsys	Shower Pipe	63,7%	RECADO [32]	1 000 €	116	

* System used for the in situ test.

Fig. 3. Obox device from Ehtech company (counter flow plates HX).

standard [31]). This value varies from 10 to 13 °C according to the standards.

– distribution mixing temperature: $T_{mix} = \mathbf{40}$°C [31–34]].

– DHW storage tank temperature: T_{tank} = [40;45;50;55;**60**;65;70;75;80;85;90]°C.

– drain water temperature: T_{drain} = [**34**;37] °C.

2.3. Benchmark

We also propose a state of the art of commercial DWHRX devices with a classification according to the type (orientation) and the technology:

The study is based on the best system currently on the market (Ehtech's Obox) [38] (see Table 2 and Fig. 3), which will also be used for the in situ test. This system is based on a counter-flow plate heat exchanger and has the particularity of incorporating a mechanical or hydrodynamic cleaning system (purge) consisting of injecting pressurized water at counter flow (network operating pressure around 3 bars) on the grey water side. We used the manufacturer's certified data for numerical applications and mainly the nominal efficiency in the "balanced case": $E_{HX} = 0{,}71$ (for $q_v = 8$ l.min^{-1}).

3. Theory on drain water recovery heat exchangers

In the case 1 (balanced configuration: $R = 1$), we can apply the NTU method to compute the nominal thermal conductance US_0:

$$NTU = \frac{US_0}{\rho c_p q_v} = \frac{E_{HX}}{1 - E_{HX}} \quad \text{with } E_{HX} = 0,71\ ;\ q_v = 8\,\text{l.min}^{-1} \tag{1}$$

$$US_0 = \rho c q_v \frac{E_{HX}}{1 - E_{HX}} = 1365\,\text{W.K}^{-1} \tag{2}$$

For the configurations 1 and 2, the HX is unbalanced and that influences the thermal conductance. Giraud et al [39] propose a correlation to compute the effective thermal conductance according to the mass flow rate on each side of a plates HX:

$$US = US_0 \frac{2q_{v_0}^{-k}}{q_v^{-k} + q_{v_{ph}}^{-k}} \text{with :}$$

$-k = 0,9$(calibrated with experimental data from Ehtech [38])

-$q_{v_0} = 8$ l.min^{-1}

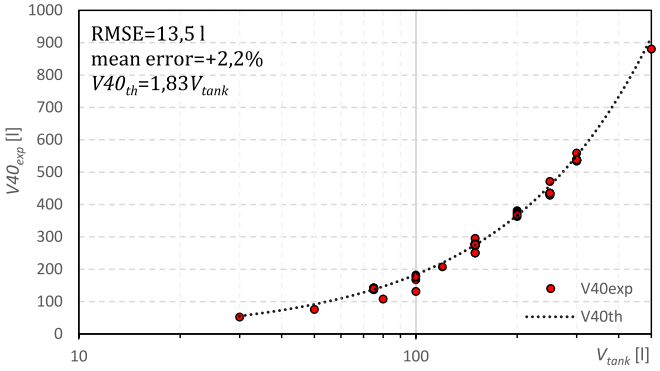

Fig. 4. V40 values from 3 manufacturers and 83 commercial electrical DHW heaters.

$$q_{v_{ph}} = \begin{cases} q_v \textit{intheconfiguration1} \\ q_{v_{cw}} \textit{intheconfiguration2} \\ q_{v_{tank}} \textit{intheconfiguration3} \end{cases} \tag{3}$$

We define for each configuration the HX exchanger efficiency as:

$$E_{HX} = \frac{T_{cwo} - T_{cwi}}{T_{drain} - T_{cwi}} \tag{4}$$

and the system efficiency which considers the heat losses between the shower head and the drain:

$$E_{syst} = \frac{P_{rec}}{P_{tot}} = \frac{\rho c_p q_{v_{ph}} (T_{cwo} - T_{cwi})}{\rho c_p q_v (T_{dhw} - T_{cwi})} = R \frac{T_{cwo} - T_{cwi}}{T_{dhw} - T_{cwi}}$$

$$\text{with} R = \frac{q_{v_{ph}}}{q_v} \text{(unbalanced factor)} \tag{5}$$

This parameter is the most important, as it considers the system as a whole, integrating losses and the fact that part of the cold water may not have passed through the HX (cases 2 and 3). For case 2 and 3 for example, the calculation leads to high HX efficiency but low system efficiency (see Figs. 7 and 8).

A final indicator is introduced, corresponding to the volume of water that can be drawn off at 40 °C, *V40*. It corresponds to the capacity of a DHW tank to produce water at 40 °C with a storage temperature at T_{dhw} (the reference is fixed at 65 °C) and a cold water at $T_{cw} = 10$ °C by following the NF EN 16147 standard on DHW heater test protocol [40]. If we assume a "piston" flow with perfect stratification and consider that

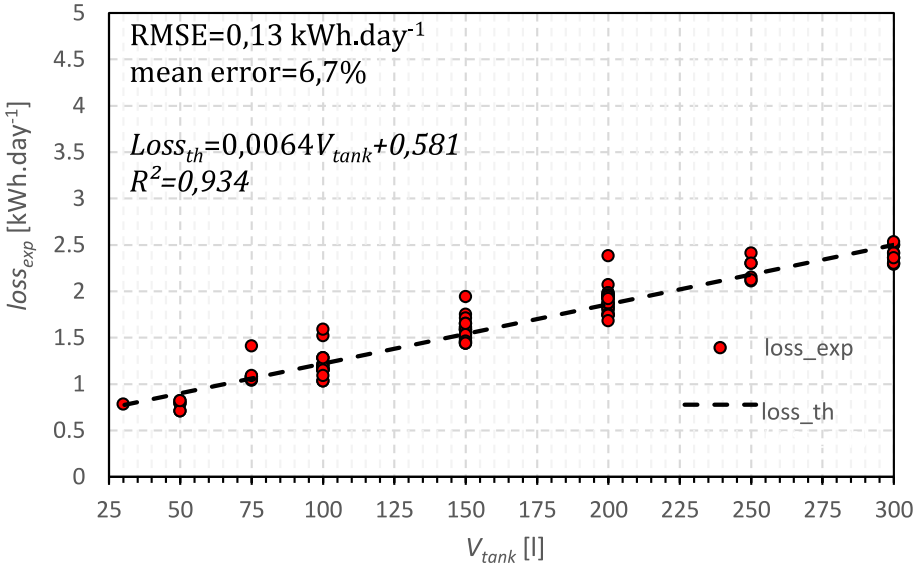

Fig. 5. Heat loss of DHW tanks from values from 3 manufacturers and 83 commercial electrical DHW heaters.

the storage tank volume V is split into 2 homogeneous isothermal volumes, hot at T_{dhw} and cold at T_{cwo} or T_{cwi} (depending on the case), then we obtain this formula for calculating $V40$:

$$V40 = V\frac{T_{tank} - T_{cw}}{40 - T_{cw}} = 1,83V \tag{6}$$

We can easily assess the accuracy of this formula by comparing the theoretical $V40_{th}$ with the normative measurements $V40_{exp}$ of 83 commercial systems from 3 different manufacturers between 30 and 500 l (see Fig. 4):

We can see that this very simple theoretical model ("piston") accurately models the V40 indicator with an average error of 2.2 % only and a root mean square error RMSE value of 13.5 l only. Stratification in this type of system is therefore quite good thanks to efficient jet breakers at the water inlet, and the overestimation of V40 due to perfect stratification is therefore negligible. Thanks to heat recovery from drain water, the cold water in the network will be preheated, enabling more hot water to be produced at 40 °C for the same DHW tank capacity. This study will quantify this gain υ40 for each configuration. This gain in production can also be converted in each case into relative savings on the volume of tank υ to be installed, on heat losses and therefore into an economic saving: on purchase and on use (less heat loss). It's hard to assess the benefits of buying a smaller DHW tank, as there is no obvious correlation from market data between the price of the system and its volume. However, we can assume that these economic gains will be negligible compared with the gains made by reducing losses and recovering heat over the system lifetime (> 20 years). For the heat losses reduction calculations, we propose the following formulae (Eq. (7) based on a benchmark of a hundred or so references from 3 manufacturers (see Fig. 5).

$$loss_{th} = 0,0064V + 0,581[\text{kWh.day}^{-1}] \tag{7}$$

3.1. Case 1: Balanced configuration

For this case, the unbalance factor is equal to 1: all the water entering the HX ends up being discharged into the shower head via the mixing valve and the DHW storage tank. Primary and secondary flow rates are therefore assumed to be equal, despite splash and evaporation losses between showerhead and drain of the order of 0.05 l.min^{-1} (i.e. less than 1 % of overall flow that is below than the flow sensor accuracy). For a counter-current exchanger with $R = 1$:

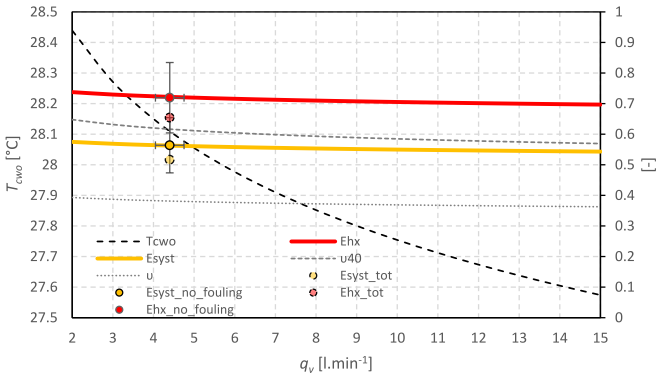

Fig. 6. Parametric study on q_v value for the balanced case (case 1) with location on in situ test results.

$$E_{HX} = \frac{T_{cwo} - T_{cwi}}{T_{drain} - T_{cwi}} \text{hence} : T_{cwo} = T_{cwi} + E_{HX}(T_{drain} - T_{cwi}) \tag{8}$$

$$E_{HX} = \frac{NTU}{1 + NTU} \text{with} NTU = \frac{US_0}{\rho c_p q_v}\left(\frac{q_v}{q_{v0}}\right)^k \tag{9}$$

The losses between the shower head and the drain are unrecoverable but degrade the overall efficiency of the system defined as the ratio between the power recovered and the maximum recoverable power:

$$E_{syst} = \frac{\rho c q_v (T_{cwo} - T_{cwi})}{\rho c q_v (T_{mix} - T_{cwi})} = \frac{T_{cwo} - T_{cwi}}{T_{mix} - T_{cwi}} \tag{10}$$

About $V40$ indicator, we can compute the $V40$ relative gain υ40 we obtain thanks to the waste heat recovery:

$$\upsilon 40 = \left(\frac{T_{tank} - T_{cwo}}{T_{mix} - T_{cwo}}\right)\left(\frac{T_{mix} - T_{cwi}}{T_{tank} - T_{cwi}}\right) - 1 \tag{11}$$

This increase in the capacity of DHW tanks to produce DHW at 40 °C thanks to waste heat recovery can be converted into a reduction in the tank volume, thereby reducing purchase costs, space requirements and heat loss. This volume gain can be calculated thanks to Eq. (12):

$$\upsilon = \frac{\upsilon 40}{1 + \upsilon 40} \tag{12}$$

We can see on Fig. 6 the performance we obtain for the balanced case on different outputs. At first, we see the significant impact on the preheating of the cold water (between 15 and 16 K). Of course, the lower the flow rate, the greater the efficiency (of the exchanger and the system) despite the drop in the *HX* exchange coefficient, even if this gain is modest. However, this drop-in flow rate reduces the power recovered, which will have an impact on the quantity of energy recovered and on profitability. A DWHRX can significantly increase the quantity of water produced by the same DHW heater (by between 55 and 65 %), and at the same time allows to install a smaller DHW heater, saving on the purchase price and, above all, on the heat losses from the tank (around 0.5 kWh of heat per day saved). However, certain activities (hairdressing, for example) or certain uses (large families) may benefit from producing more hot water with the same storage volume. We plotted the results of the in-situ test (see §V) by considering global results considering transient phases and fouling phenomena and nominal results dismissing transient and fouling effects. The nominal results follow the theory, and the fouling effects seem to have a significative impact on the DWHRX performance (nominal efficiency reduced of about 10 %).

3.2. Case 2: Unbalanced configuration with connection to the mixing valve

Here, the HX is unbalanced ($R \leq 1$): only part of the cold water enters the exchanger primary side, with the storage tank connected directly to the cold water network (see Fig. 2). The unbalance factor must be determined for each configuration. However, the total flow is discharged at the exchanger secondary side (drain water). The flow rate of preheated water will therefore depend on the total flow rate required and above all on the temperature of the stored water in the tank: the hotter the DHW water, the greater the demand on the heat exchanger to preheat the cold water at the mixing valve. A mass balance and an enthalpy balance at the mixing point between the cold water and the hot water in the storage tank are carried out, balances that are combined with the NTU theory:

$$R = \frac{\rho q_{vcw} c_p}{\rho q_v c_p} = \frac{q_{vcw}}{q_v} = \frac{T_{mix} - T_{tank}}{T_{cwo} - T_{tank}} \tag{13}$$

$$q_{vcw} = q_v \frac{T_{mix} - T_{tank}}{T_{cwo} - T_{tank}} \tag{14}$$

$$US = US_0 \frac{2q_{v_0}^{-k}}{q_v^{-k} + q_{v_{cw}}^{-k}} \tag{15}$$

$$NTU = \frac{US}{\rho c_p q_{vcw}} = \frac{US_0}{\rho c_p q_v} \left(\frac{2q_{v_0}^{-k}}{q_v^{-k} + q_{v_{cw}}^{-k}} \right) \left(\frac{T_{cwo} - T_{tank}}{T_{mix} - T_{tank}} \right) \tag{16}$$

The temperature of the preheated water is obtained thanks to the formulas of the efficiency of the exchanger (NTU methods and definition via temperatures):

$$E_{HX} = \frac{1 - exp[-NTU(1-R)]}{1 - Rexp[-NTU(1-R)]} = \frac{T_{cwo} - T_{cwi}}{T_{drain} - T_{cwi}} \tag{17}$$

We obtain a nonlinear equation we can simply solve by using iterative methods by the following algorithm:

$$T_{cwo} = T_{cwi} + E_{HX}(T_{cwo}; T_{tank}; q_v)(T_{drain} - T_{cwi}) = f(T_{cwo})$$

$$T_{cwo}^{n+1} = f(T_{cwo}^{n}) \tag{18}$$

Finally, we can calculate:

$$E_{syst} = \frac{\rho c_p q_{vcw}(T_{cwo} - T_{cwi})}{\rho c_p q_v (T_{mix} - T_{cwi})} = R\left(\frac{T_{cwo} - T_{cwi}}{T_{mix} - T_{cwi}} \right) = \left(\frac{T_{mix} - T_{tank}}{T_{cwo} - T_{tank}} \right) \left(\frac{T_{cwo} - T_{cwi}}{T_{mix} - T_{cwi}} \right) \tag{19}$$

About ʊ40 and ʊ indicators, we can use the same equations given for the case 1 (Eq. (11) and (12).

Firstly, we can see that compared with the other 2 cases, this set-up is the most efficient in terms of DHW production at 40 °C (*V40* indicator) because it almost doubles this indicator (+80 to 90 %), which could be interesting in certain cases (hairdressing salons, large families). With the same *V40*, this means that a more compact tank (about 2 times smaller) can be used to produce the same amount of hot water at 40 °C, which could be advantageous in some cases (small apartments/constrained or reduced spaces). This potential reduction in volume can save around 0.6 kWh per day in heat loss, or around 200 kWh and €50 in savings per year. Secondly, the heat exchanger has very good efficiencies (between 80 and 85 %) due to an unbalanced flow rates. However, not all the cold water needed to produce DHW passes through the exchanger (the tank receives cold water directly from the district network, see Fig. 2), which reduces overall efficiency to around 45 % (a loss of 20 % compared with the balanced configuration). However, this configuration is necessary, particularly in the case of collective production by accumulation, where it is impossible to connect to the storage tank but only to the mixing valve.

3.3. Case 3: Unbalanced configuration with connection to the tank

In case 3: the HX is also hydraulically unbalanced ($R < 1$): part of the cold water only enters the primary of the HX since the mixer is directly connected to the cold water of the network (see Fig. 2). It will therefore be necessary to determine the unbalanced factor for each configuration. However, the total flow is evacuated to the secondary side of the exchanger. The preheated water flow will therefore depend on the total flow required and above all on the tank water temperature: the hotter the DHW water will be and the less the exchanger will be used for preheating from cold water to the mixer. A mass balance and an enthalpy balance at the mixing point between the cold water and the hot water of the tank (at the thermostatic tap) is carried out, which is combined with the NTU theory:

$$R = \frac{\rho q_{vtank} c_p}{\rho q_v c_p} = \frac{q_{vtank}}{q_v} = \frac{T_{mix} - T_{cwi}}{T_{tank} - T_{cwi}} \tag{20}$$

$$q_{vtank} = q_v \frac{T_{mix} - T_{cwi}}{T_{tank} - T_{cwi}} \tag{21}$$

$$US = US_0 \frac{2q_{v_0}^{-k}}{q_v^{-k} + q_{v_{tank}}^{-k}} \tag{22}$$

$$NTU = \frac{US}{\rho c_p q_{vtank}} = \frac{US_0}{\rho c_p q_v} \left(\frac{2q_{v_0}^{-k}}{q_v^{-k} + q_{v_{tank}}^{-k}} \right) \left(\frac{T_{tank} - T_{cwi}}{T_{mix} - T_{cwi}} \right) \tag{23}$$

The temperature of the preheated water is obtained thanks to the formulas of the efficiency of the exchanger (NTU methods and definition via temperatures):

$$E_{HX} = \frac{1 - exp[-NTU(1-R)]}{1 - Rexp[-NTU(1-R)]} = \frac{T_{cwo} - T_{cwi}}{T_{drain} - T_{cwi}} \tag{24}$$

We obtain finally:

$$T_{cwo} = T_{cwi} + E_{HX}(T_{drain} - T_{cwi}) \tag{25}$$

$$E_{syst} = \frac{\rho c_p q_{vtank}(T_{cwo} - T_{cwi})}{\rho c_p q_v (T_{mix} - T_{cwi})} = R\left(\frac{T_{cwo} - T_{cwi}}{T_{mix} - T_{cwi}} \right) = \frac{T_{cwo} - T_{cwi}}{T_{tank} - T_{cwi}} \tag{26}$$

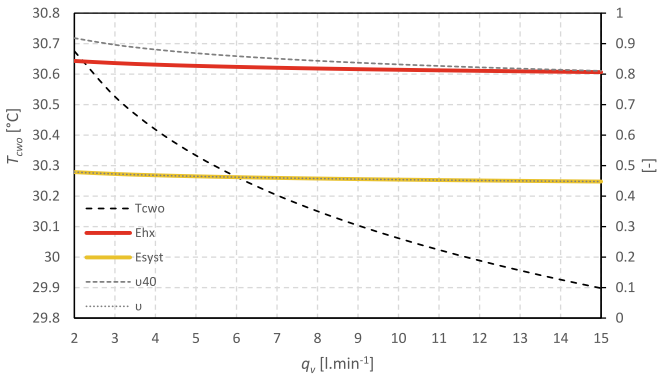

Fig. 7. Parametric study on q_v value for the unbalanced case connected to the mixing valve (case 2).

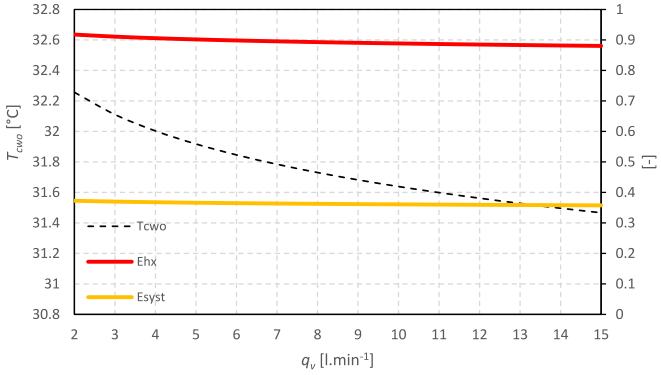

Fig. 8. Parametric study on q_v value for the unbalanced case connected to the tank (case 3).

Here, we are not calculating the indicators linked to the *V40*, as the cold water reaching the mixer does not benefit from preheating, so this will have no impact on this indicator compared to the reference case (without DWHRX). On the other hand, the DHW tank, supplied with preheated water, will consume less energy to produce DHW (and will run for less time).

Firstly, we can see that compared with the other 2 cases, this set-up produces the hottest preheated water at the outlet of the HX up to 32 °C with the highest HX efficiency (around 90 %) due to unbalanced flow rates. However, not all the cold water needed to produce DHW passes through the exchanger (the mixing valve receives cold water from the network, see Fig. 2), which reduces overall efficiency to around 35 % (a decrease of 35 % compared with the balanced configuration). For a standard storage tank temperature of 65 °C, this configuration is therefore the least efficient. However, it is sometimes the only one that is technically possible, particularly in collective buildings where grey water recovery is centralized in a unique large system, for example. Finally, this configuration will not improve the *V40* indicator and will therefore not reduce losses (static losses), so the initial storage volume should be retained.

3.4. Comparison between the 3 configurations

Fig. 9 compares the 3 configurations according to the tank temperature.

The double connection (case 1) offers the highest efficiencies whatever the storage temperature, which is expected since even though the flow to the mixing valve and the flow to the storage tank will vary according to the storage temperature, the overall flow will pass to the exchanger primary side. The simple connection to the mixing valve offers stable performance for storage temperatures above 55–60 °C: temperatures that destroy or at least prevent the development of legionella. For higher storage temperatures, which could occur with the use of a biomass boiler for example, the efficiencies obtained tend towards the efficiencies of the double connection, which is logical since little hot water from the tank is needed to obtain water at 40 °C with cold water preheated to around 30 °C. Most of the flow will pass through the exchanger. On the other hand, this configuration is not suitable for thermodynamic storage tanks, which need to limit storage temperatures to optimize the coefficients of performance of the heat pumps. Nor will it be suitable for undersized or scaled storage tanks, which will cool down quickly or fail to reach their set points, which will reduce the efficiency of the exchanger as the water is drawn off: if the storage water approaches 40 °C, most of the flow will pass through the tank and no longer through the exchanger. Simple connection to the mixing valve makes sense when we want to maximize the *V40* index or when the DHW is based on collective storage where it will be impossible to connect to the storage tank too far away. Finally, the single connection to the

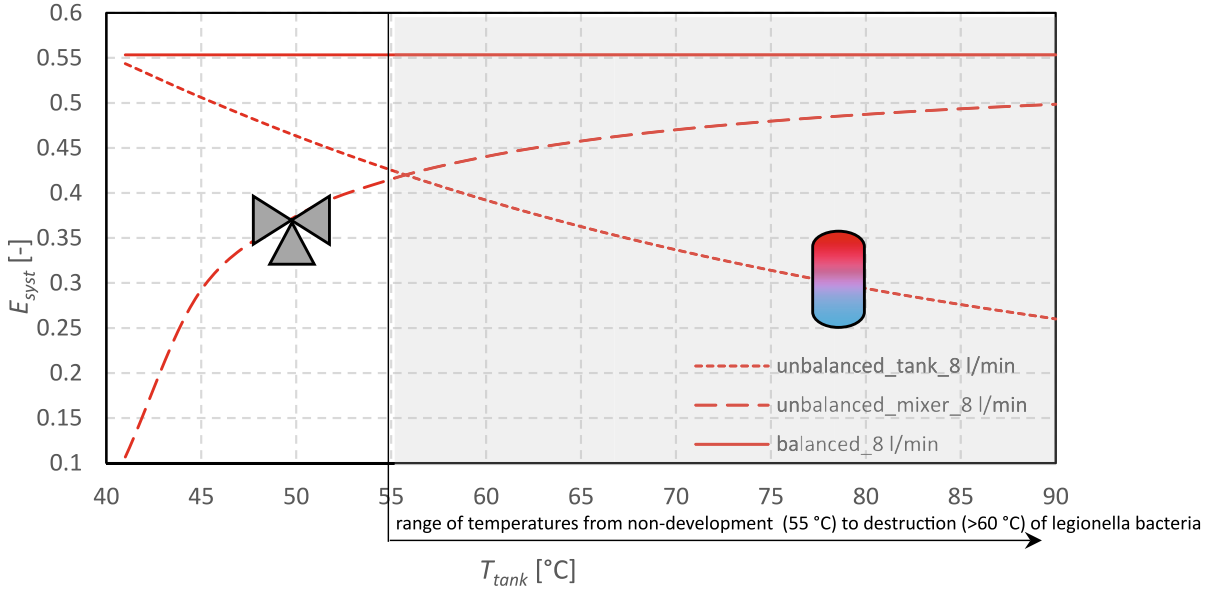

Fig. 9. Comparison of E_{syst} between the 3 cases according to T_{tank} (for q_v = 8 l.min^{-1} and T_{drain} = 34 °C).

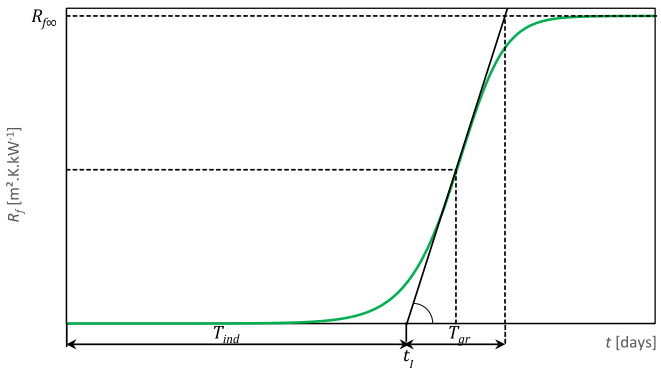

Fig. 10. Nebot biofilm modeling approach.

storage tank is only effective for low storage tank temperatures. Efficiency drops rapidly and is the lowest compared to the other configurations for normal storage temperatures storage temperatures, i.e. above 55 °C.

4. Theory on heat exchanger fouling

The in situ study showed a significant impact linked to fouling on the "grey water" side due to the various elements contained in the grey water (soap, epidermis, body fluids) as well as the presence of oxygen due to a pipe that is not under load. The dynamics observed correspond to the development of a biofilm feeding on this organic matter in an aquatic environment and in the presence of oxygen. Various models exist for modelling the thermal resistance of fouling in relation to this biofilm development. Various authors have already worked on the fouling of heat exchangers, mainly for fouling problems in hot water circuits (DHW or heating) [41] or for seawater exchangers [42] or cooling circuits [43]. Others have also studied these fouling resistances on heat exchangers using sewage water [44,45]. Very few studies have focused specifically on fouling in grey water heat exchangers and, more specifically, on fouling in shower water heat exchangers. Only Grundén et al [26] have set up an experimental protocol to attempt to assess this, but with poor results. Shen et al [28–30] worked on a heat pump assisted by shower drain water and was able to characterise the fouling dynamics in relation to the development of a biofilm. Various models exist to simulate the development of a biofilm on the exchange surface of a heat exchanger. There are the historical models of Kern (exponential) [46]

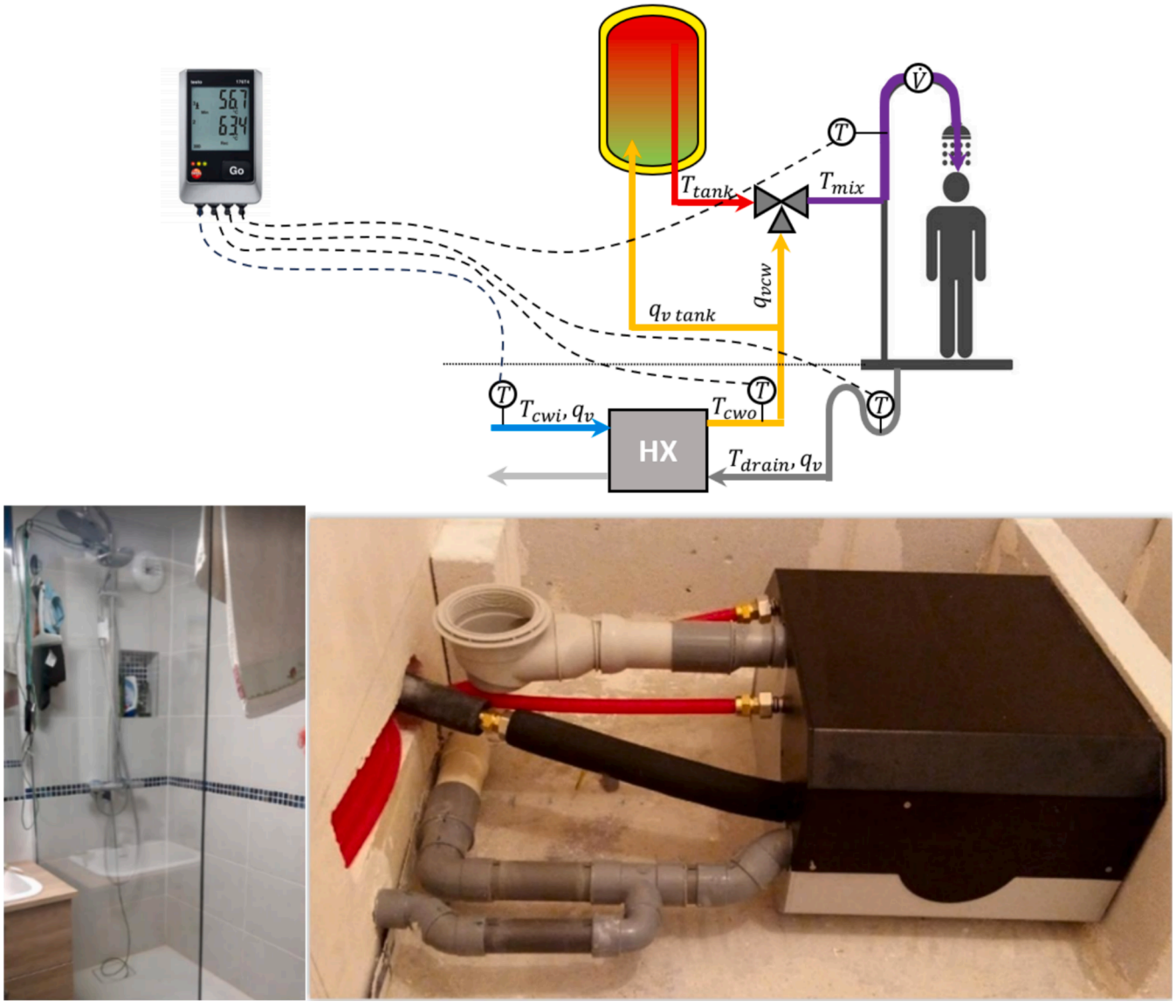

Fig. 11. Sensor location and photo of the tested device.

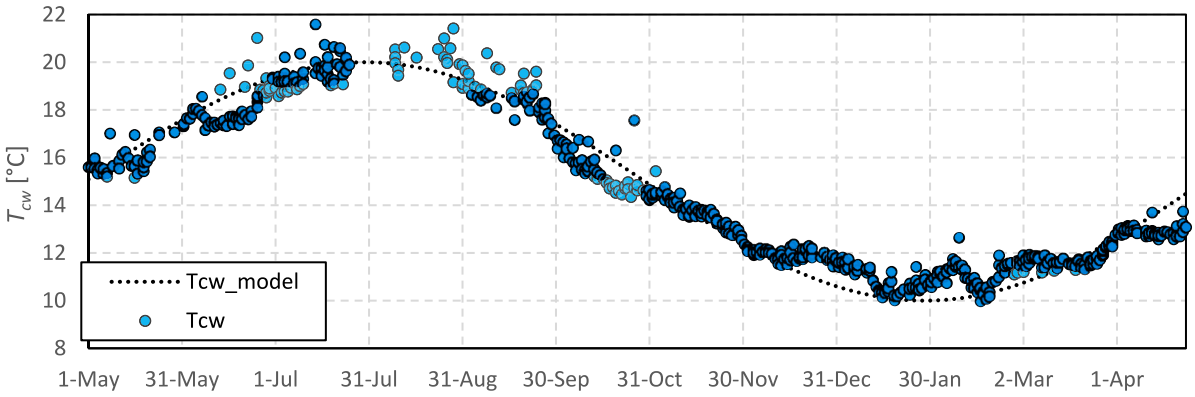

Fig. 12. District network cold temperature (measurements and modeling).

and of Konak, which introduces asymptotic fouling based on the concept of a driving force for the development of deposits [47]. Finally, more recently, Nebot [48] has proposed an adaptation of Konak's model to reproduce "S-curve" dynamics with an induction phase T_{ind}, an exponential growth phase T_{gr} and a stabilization phase (see Fig. 10) with a fouling thermal resistance that stabilizes at $R_{f\infty}$. This model has been used by many authors mainly to study the best way to clean the heat exchangers [49].

$$\begin{cases} \dfrac{dR_f}{dt} = k_f\left(R_{f\infty} - R_f\right)R_f \\ R_f(0) = R_{f0} \neq 0 \end{cases}$$

$$t_I = t\text{such as}\frac{d^2R_f}{dt^2} = 0 \leftrightarrow R_f = \frac{R_{f\infty}}{2} \tag{27}$$

We define the growth time T_{gr} and the induction time T_{ind}:

$$T_{ind} = t_I - \frac{1}{k_f\frac{R_{f\infty}}{2}}\text{and}T_{gr} = \frac{1}{k_f\frac{R_{f\infty}}{4}} \tag{28}$$

We define the fouling thermal resistance R_f such as:

$$R_f = \frac{1}{US_f} - \frac{1}{US_{corr}} = \frac{1}{US_f} - \frac{1}{US_0\left(\frac{q_{vnom}}{q_v}\right)^{-k}}\text{with}US_0 = US\left(\frac{q_{v0}}{q_{vnom}}\right)^{-k}$$

With:

q_{v0} : *volume flowr ate of the shower used to determine the reference thermal conductance*

$$q_{vnom} = 8\text{l.min}^{-1} \tag{29}$$

5. In situ tests

5.1. Metrology and measurement protocol

A heat recovery unit has been installed in a flat for a family of 3 people (2 adults and a small child (<1m)) in an urban context (Strasbourg, France). The technical installation consisted of DHW production using a 200 l electric water heater tank (Joule effect), and an Ehtech Obox heat recovery unit [39] (see Fig. 11) connected to both the DHW tank and the thermostatic mixing valve installed directly under the shower tray. The distance between the drain and the recovery unit is very small (30 cm) and has been thermally insulated. A thermostatic mixer adjusts the temperature according to the set point (around 40 °C in practice) and according to the temperature at the outlet of the heat recovery unit. In terms of metrology, we used type K thermocouples to measure the temperatures of cold water T_{cwi}, preheated water T_{cwo}, water drawn off at the shower head T_{mix} and water at the drain T_{drain} (see Fig. 11). A data logger with a 6 s time step was used. The sampling frequency was set as low as possible in order to capture dynamic regimes, in particular temperature rises at start-up. These thermocouples have been tested beforehand in a controlled water bath to be calibrated and to select the best sensors, the important thing here being that the temperature differences are measured as accurately as possible. In addition, in situ blank tests using cold water only were carried out to check that the 4 temperature sensors were working properly (in this case, they should give the same value) and to check that there were no measurement drifts.

The flow and volume sensor was calibrated by comparing the measurements with a global mass measurement (measurement of the final mass of water drawn off). A dozen withdrawals of between 10 and 40 L were carried out for flow rates varying from 2 to 10 l.min^{-1}, and an average error of + 2 % was calculated between the flow meter and the global mass measurements.

5.2. Experimental results

i. District cold temperature

Firstly, the temperature of the cold water in the public network was measured at the hydraulic collector approximately 1 m upstream of the heat recovery unit. It turns out that the in situ test was carried out in a dense urban environment (in the city center of Strasbourg, France), which generates high average temperatures of around 15 °C due to urban heat island phenomena in particular, compared with around 12 °C in a rural environment (the French regulation sets at 12,8 °C the mean value of district cold water for DHW calculations) (see Fig. 12). Most authors use values ranging from 10 to 12 °C [7,9,34] for their studies. The seasonal variation of this temperature can be satisfactorily modeled by a sinusoidal law (see eq. (30). The final amplitude is therefore of the order of 10 K, varying between 10 and 20 °C. The amount of energy recovered will also vary with the same dynamics and will therefore be greater in winter than in summer. It is therefore important to ensure that the system is running properly before the winter period (maintenance

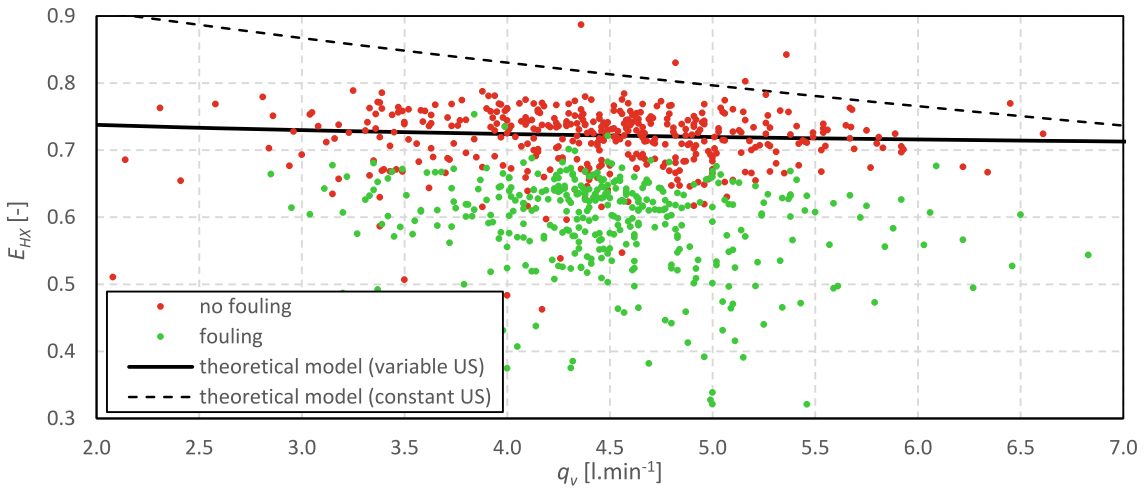

Fig. 13. Average exchanger efficiency per shower as a function of DHW shower flow rate.

operations: thermal, chemical or mechanical cleaning), to maximize recovery during this cold period. The level of recovery will also depend on the climate, as the average temperature of the water in the network is directly correlated to the outside temperature (as the network is buried in the ground, damping and phase-shifting phenomena tend to bring the temperature towards the average annual temperature at any depth). The performance of such systems will therefore need to be verified according to the concerned climatic zone.

$$T_{cw} = T_m + \Delta T sin\left(\frac{2\pi}{365}t\right) (\text{with} t = 0 \text{corresponds to the 1st of May})$$

$$\text{With } T_m = 15^{\circ}C \text{ and } \Delta T = 5\,K \tag{30}$$

ii. DHW temperature

The DHW temperature measured at the shower head corresponds to the usual values (regulatory and measured in various studies), i.e. 40 °C.

iii. Drain water temperature

The drain temperature has been measured by an immersed thermocouple sensor. It turns out that this data is essential to characterize the recoverable energy deposit and to characterize the performance of heat recovery systems. Ideally, this temperature should be as high as possible.

In practice, the water exiting the shower head undergoes various heat exchanges that cause its cooling:

– evaporation loss, initially due to the sudden drop in pressure.

–evaporation loss between the film of water on the surface of the skin and between the water droplets in suspension and the surrounding air. This evaporation depends mainly on the level of humidity and the air temperature in the room.

–losses by convection between the film of water on the skin, the air and the skin

–convection losses between suspended water droplets and the air.

The literature establishes these losses between 10 and 20 % of incident energy, with drain temperatures varying between 33 and 37 °C [5,6,7,9] (with a DHW temperature of 40 °C at the shower head). Test standards, on the other hand, are more favorable, assuming losses of the order of 0 to 10 % with drain temperatures ranging from 37 °C [32,34] to 40 °C (no loss) [31,33,34] (see Table 1). It turns out that in this in situ test, 2 values were distinguished: 33 °C for adults and 36 °C for children. In fact, it was necessary to differentiate this drain temperature value for adults and children, which turned out to be significantly different, probably due to a difference in waterfall height (shorter water suspension time for children) and a difference in corpulence (shorter body exchange surface). On average, for this in situ tests, the unrecoverable part of the incident DHW heat reaches 21 % on average (see Fig. 1).

iv. Heat exchanger efficiency and preheating water temperature

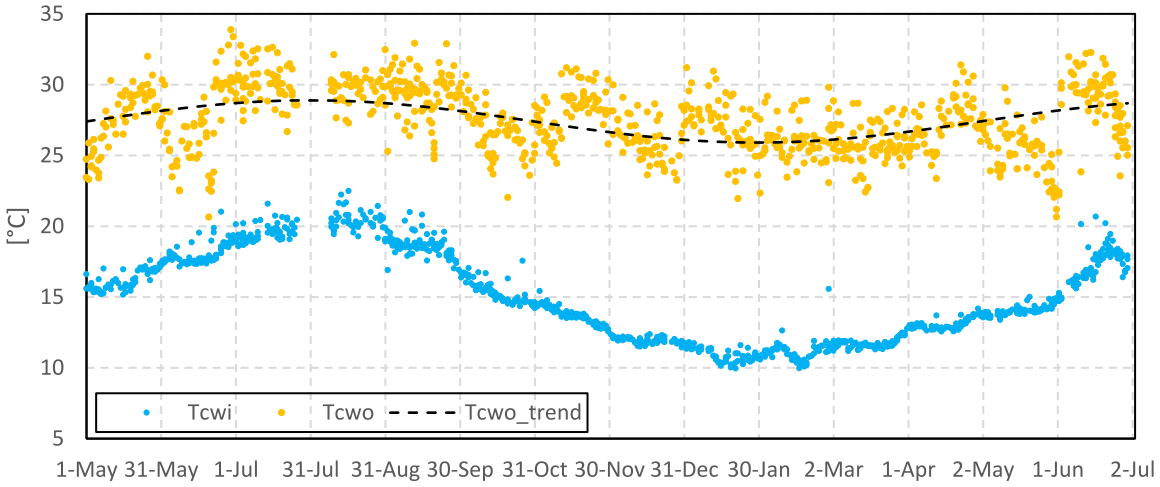

Fig. 14. Inlet (T_{cwi}) and mean outlet (T_{cwo}) temperatures of the heat exchanger.

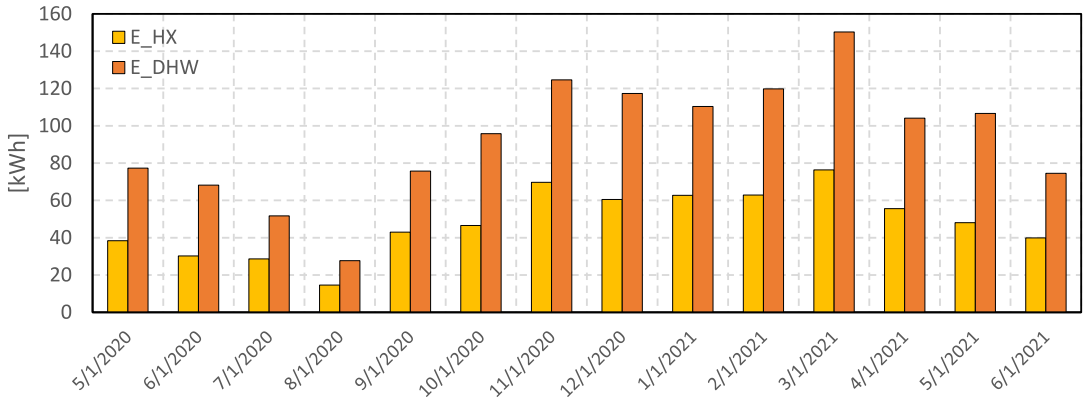

Fig. 15. Comparison between DHW energy consumption (E_{DHW}) and DHW heat recovery (E_{HX}) over 1 year.

The efficiency of the heat exchanger E_{hx} is classically defined by the temperatures at its terminals (see Eq. (8). The average efficiency of the heat exchanger is calculated using the average value on the efficiency computed at each time step. Also, the so-called system efficiency E_{syst} will be calculated in relation to the DHW temperature and will integrate the losses between the shower head and the drain (see Eq. (10).

The nominal efficiency given by the manufacturer is 71 % for a nominal DHW mass flow rate of 8 l.min^{-1}. Fig. 13 plots the average efficiencies E_{hx} per shower over the test period (14 months), distinguishing cases where the exchanger was clogged and cases where it was operating under nominal conditions (unclogged). The "fouling periods" were detected by means of a filter on the values obtained: from a certain deviation from the theoretical nominal value (90 %), the exchanger is deemed to be clogged. It can be seen that the flow rate has little impact on exchanger performance, which is contrary to the theory of the number of NTU transfer units. The proposed model (*cf* §III and Eq. (3) from Giraud [39] will take this effect into account. The average efficiency of the recovery HX is therefore relatively constant regardless of flow rate, and the impact of fouling on performance is noticeable despite weekly hydromechanical purging. The annual average efficiency of the exchanger is 0.66 for a nominal efficiency of 0.71 at average flow rate (4.1 l.min^{-1}). Performance losses due to fouling therefore average 8 %. The system efficiency including losses between the mixing valve and the drain is 0.52, which means that DHW consumption has been divided by a factor of 2. This result shows that this system offers performance equivalent to a thermodynamic water heater with an usual value for the heat pump coefficient of performance COP of 2 [50] or a solar system, the heat coverage rates of which in France vary between 40 and 60 % depending on the climatic zone [50].The loss factor (non-recoverable part of DHW) is 21 % on average.

The preheating temperature T_{cwo} at the outlet of the HX is assumed to follow the dynamics of the cold water temperature T_{cwi}. Fig. 14 shows the annual variations of these 2 temperatures at the terminals of the recovery exchanger. However, mainly due to fouling phenomena, but also to unsteady phenomena (short withdrawal time for example), the water temperature at the exchanger outlet varies in a dispersed manner even if the same sinusoidal trend can be seen by plotting a sinusoidal trend curve obtained thanks to an optimization procedure. However, it varies from a minimum of 20 °C to temperatures of up to 34 °C, with an average of around 28 °C. Artificially, heat recovery from drain water therefore enables virtually cold water to be recovered at much higher temperatures than the real district network water temperature. The heat exchanger raises this temperature by around 10 K (summer operation) to around 20 K (winter operation).

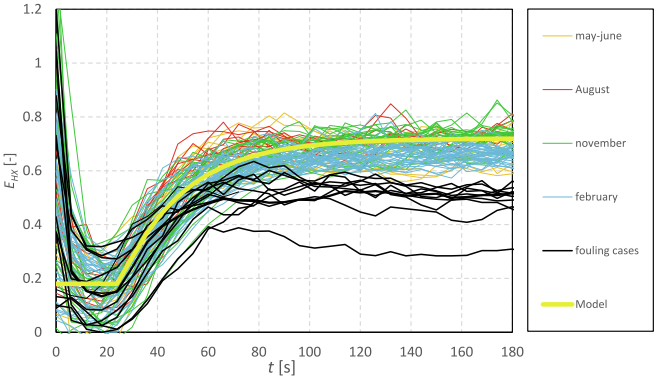

Fig. 16. Evolution of HX efficiency according to season and degree of fouling.

v. Energy

The energy recovered during this in situ test amounts to 589 kWh. yr^{-1}, i.e. a significant gain in terms of final energy of 7 kWh$_{FE}$.m^{-2}.yr^{-1} (or 16 kWh$_{PE}$.m^{-2}.yr^{-1} in primary energy) here in the French context. This corresponds to savings of around €120/year (2021) for an initial investment of around €1,000. This is probably one of the most cost-effective ways of significantly reducing a home's primary energy consumption without subsidies and heavy renovation works. As already mentioned, the performance of this type of system is seasonal, and heat recovery is most effective in winter when cold water temperatures are lowest (see Fig. 15).

vi. Dynamics

The dynamics of this system were then studied to assess the impact of unsteady effects on its performance, and in particular to analyze the impact of DHW withdrawal time. Firstly, one conclusion is that there is no obvious effect of seasonality (cold water temperature, ambient temperature and humidity in bathroom) or the level of fouling of the exchanger on the time response of the exchanger. This is shown in Fig. 16 by plotting various withdrawal cycles during each season with and without clogged exchangers. As it turns out, the system's inertia is relatively low, enabling it to heat up rapidly. In Fig. 16, we can see various evolutions at different times of the year of the HX efficiency, which can be likened to a first-order function with delay. The delay is mainly due to the fact that hot water must take a certain uncompressible

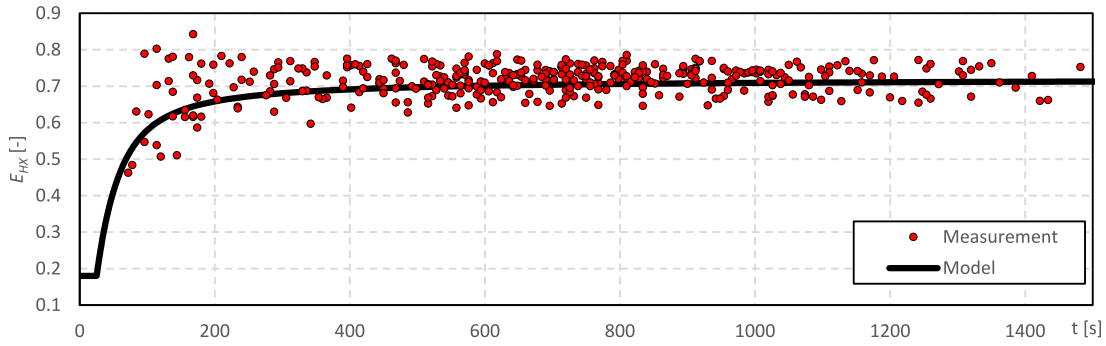

Fig. 17. Mean value of HX efficiency on each shower according to the shower duration for unclogged HX.

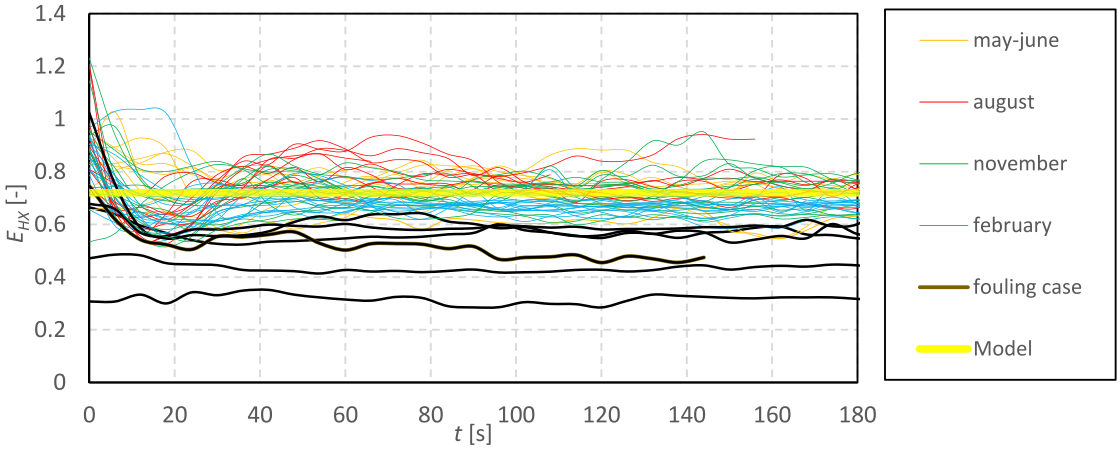

Fig. 18. Evolution of HX efficiency according to season and degree of fouling for successive showers (HX preheating).

time to flow through the network between the storage or production point (DHW tank, boiler) and the extraction point. This time is specific to each installation. Here, the length of the network is short (about 1 m), so that this dead time is relatively short, estimated at 25 s on average (between 10 and 30 s). The time constant has also been estimated at 25 s on average, which means that the 95 % response time corresponds on average to a time of about 100 s. This time is ultimately less than the average DHW withdrawal time of 727 s here (12 min). Also, at start-up, the water stagnates in the network, generally at a temperature close to ambient temperature, which is higher than the network cold water temperature. In practice, this artificially generates non-zero start-up efficiencies of the order of 10 to more than 100 % in some favorable cases (see Fig. 16). The following dynamic model is proposed to simulate the behavior of a shower water recovery heat exchanger (without fouling) (see model on Fig. 16):

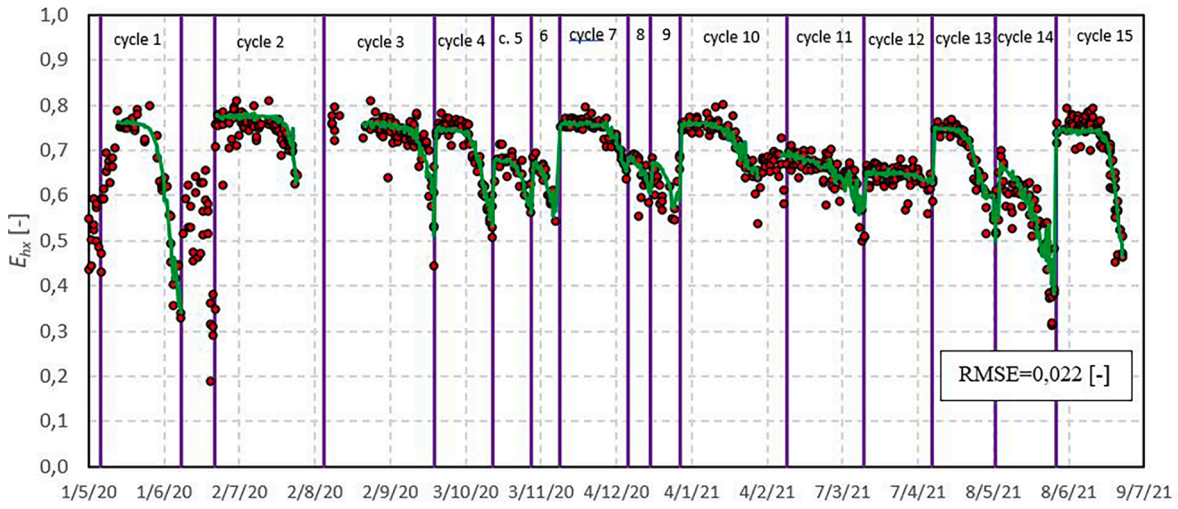

Fig. 19. Evolution of HX efficiency over the time (14 months), chemical purge planning and fouling modeling (green curve). (For interpretation of the references to colour in this figure legend, the reader is referred to the web version of this article.)

Table 3
Sensor characteristics.

Physical quantity	Technology	Accuracy	reference
temperature	Armoured Type K Thermocouple	∓0,6 K	Data logger Testo 176 T4
Water volume	Blades sensor	∓8 %	Amphiro b1connect

$$E_{hx} = f.E_{hx}^{SS} \text{ with } f = \text{MAX}\left(0,25; 0,25 + 0,75\left(1 - e^{-\frac{t-t_r}{\tau}}\right)\right)$$

$$\text{and } E_{hx}^{SS} = 0,71; t_r = 25s \text{and } \tau = 25s \quad (31)$$

In practice, a coefficient C_{dyn} can be calculated to characterize this transient effect:

$$C_{dyn} = \frac{E_{hx}}{E_{hx}^{SS}} \text{with} E_{hx}^{SS} \text{the steady state HX efficiency (or nominal value)} \quad (32)$$

C_{dyn} coefficient compares the average efficiency over a whole withdrawal cycle with the steady-state efficiency. In practice, this coefficient averages 0.97, in line with standards tests carried out on certain equivalent systems [32,39]. For the same system (Obox from Ehtech), laboratory tests measure a value of 0,95 [39]. This means at first that unsteady-state effects have a negligible impact on performance, and that modeling via a fixed efficiency assuming steady state remains a good approximation. However, depending on the user and draw-off profile, and in particular for short draw-offs (< 240 s), this impact will still need to be verified. On Fig. 17, the mean HX efficiency of each shower is plotted according to the shower duration (in the no fouling case). We see after about 240 s (4 min), we reach 95 % of the nominal value. Finally, in some cases, the fact that several showers are taken at the same time (morning or early evening) means that the heat exchanger has already been preheated for the following showers. The cold water is thus already preheated, sometimes to significant levels due to stagnation (close to T_{drain}), which generates different dynamics with dynamic coefficients C_{dyn} close to or even greater than 1 (see Fig. 18). This phenomenon concerns about 1/3 of showers and contributes in practice to obtain C_{dyn} coefficients slightly higher than those calculated in standards which do not consider this phenomenon (see Fig. 18) (0,97 here vs 0,95 for the standard test). In this case, a good model is to simply consider a constant value for the HX efficiency which can vary according to the fouling rate.

vii. Heat exchanger fouling analysis

Finally, a fouling analysis was carried out and a numerical model has been developed. Fig. 19 shows that the fouling cycles characteristic of biofilm development are put in place (see §IV), characterized by an induction phase (stable efficiency for several weeks (between 1 and 3 weeks)), followed by a growth phase in which the efficiency of the exchanger decreases almost linearly. The stabilization phase is never really observable here because of fairly regular purging. Nebot's model [48] (see Fig. 10 and Eq. (27) was implemented using a numerical method of the Euler type, taking into account a correction for the withdrawal rate (see Eq. (29). The parameters were then determined using an optimization method aimed at reducing the Root Mean Squared Error RMSE between model and measurements on HX efficiency E_{hx} value for each fouling cycle. The parameters of the Nebot model are given in Table 3. Average values are also given at the end of Table 3. A few comments can be made from this analysis. Firstly, for each cycle (15), the parameters are significantly different, suggesting that certain parameters undoubtedly have an influence on the dynamics of fouling and biofilm development (cold water temperature, average exchanger temperature, physiochemical composition of grey water (potentially different between winter and summer (more sweating), shower frequency, shower duration, etc.). In addition, it would appear that the heat exchanger clogs up more quickly and to a greater extent during hot periods. But these observations have yet to be confirmed. As a reminder, on average in this particular case (about weekly mechanical purges and monthly chemical purges), fouling reduces nominal efficiency by around

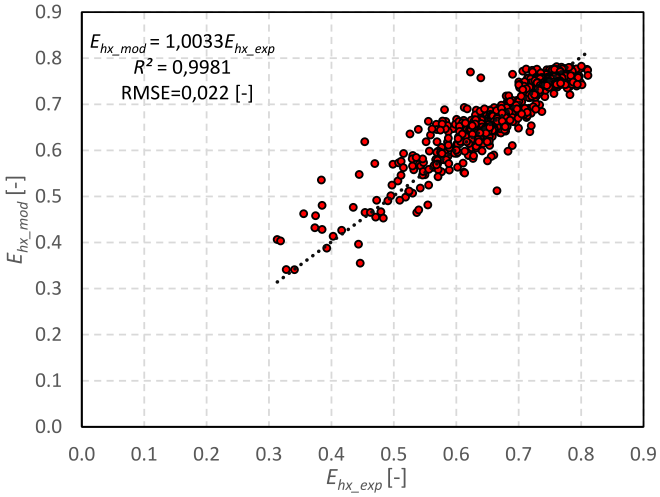

Fig. 20. Model HX efficiency vs experimental efficiency.

Table 4
Nebot model parameters for fouling cycles.

		$R_{f,0}$	$R_{f\infty}$	k_f	US_0	US_∞	NTU_∞	E_{hx_∞}	RMSE	T_{cw}
Cycle number (see Fig. 19)	1	0,002	5,47	0,082	1712	165	0,30	0,23	0,022	16
	2	1,03E-06	8,17	0,067	1806	115	0,21	0,17		19
	3	0,00044	12,41	0,026	1632	77	0,14	0,12		19
	4	0,00023	1,56	0,36	1551	453	0,81	0,45		17
	5	0,00082	0,77	0,96	1109	596	1,07	0,52		15
	6	0,046	1,19	0,47	1117	479	0,86	0,46		14
	7	3,90E-05	1,13	0,42	1652	575	1,03	0,51		13
	8	0,03402	2,16	0,18	1135	329	0,59	0,37		12
	9	0,00254	0,65	2,43	1051	625	1,12	0,53		12
	10	0,00069	0,84	0,41	1645	692	1,24	0,55		11
	11	0,0312	2,99	0,04	1192	261	0,47	0,32		11
	12	0,00098	0,48	0,48	978	665	1,19	0,54		12
	13	0,00108	1,46	0,32	1576	478	0,86	0,46		13
	14	0,11299	7,36	0,02	1120	121	0,22	0,18		15
	15	4,80E-06	2,98	0,24	1120	258	0,46	0,32		17
	Mean	0,0073	1,1	0,19	1433	556	1,00	0,50	0,067	15
		$m^2.K.kW^{-1}$	$m^2.K.kW^{-1}$	$kW.m^{-2}.K^{-1}.d^{-1}$	$W.K^{-1}$	$W.K^{-1}$	–	–	–	°C

8 %. In a case where no chemical purging is carried out. It is possible that this coefficient could reach around 50 %, given the results observed. These values are consistent with the work of Shen et al [28–30] who were able to show similar values over a period of several weeks on an immersed coil type exchanger (natural convection outside the pipe, without purging) with a reduction of the order of 20 to 30 % of the heat transfer and an induction phase of the order of 1 week. Finally, in some cases, despite chemical purging, the heat exchanger remains partially clogged (see in particular cycles 5, 6, 8,9, 11, 12 or cycle 14). Studies are still needed to better understand the phenomena of purging, whether mechanical, chemical or thermal, in order to make it more effective.

In the literature, only Shen et al [28–30] provide experimental data on the final fouling resistance $R_{f\infty}$ for a heat exchanger in contact with shower water. In particular, they arrive at an $R_{f\infty}$ value of 0.53 m^2.K.kW^{-1}, which is close to our average model (1.1 m^2.K.kW^{-1}) (see Table 4), bearing in mind that these values vary from 0,48 to 12,4 m^2.K.kW^{-1} depending on each cycle. In addition, we also found similar results to Shen et al [28–30] on the reduction in heat transfer of the order of 20 % on average and on fouling dynamics (induction period of a few days and growth periods of a few weeks) (see Table 4). Finally, Fig. 20 shows the good overall correlation between the model and experimental data for the 15 fouling cycles identified.

6. Conclusion

Heat recovery is therefore a relatively simple and effective way of significantly reducing energy consumption in residential buildings (individual or collective), as well as in certain tertiary buildings (hotels, hairdressing, sports facilities). This work began with a review of the state of the art in terms of standards for this type of heat exchanger, followed by a review of existing shower water heat recovery systems and their classification. Then this work proposes original theoretical, analytical and numerical models to characterize the performance of this type of system, taking into account the hydraulic connection configuration, flow rate variation, unsteady effects and the effects of exchanger fouling. Several performance indicators were evaluated, starting with the efficiency of the heat exchanger, but also the efficiency of the system integrating heat losses between the shower head and the drain, and the *V40* indicator: the volume of water that can be produced at 40 °C by a given volume of DHW tank. The in situ test enabled the models to be calibrated, particularly with regard to fouling and unsteady effects, and also validated the high performance of this type of system in a residential building, with a system efficiency of 52 % over one year, i.e. a 2-fold reduction in DHW consumption. The in situ test enabled us to quantify the impact of heat exchanger fouling, which proved to be non-negligible (of the order of 8 %, equivalent here to 5 efficiency points), and showed that test standards could be improved to take better account of the effects of fouling, to better assess heat loss in a shower (drain temperatures level are overestimated compared to reality) and to better take into account dynamic effects, notably by considering the succession of showers (which concerns almost 1/3 of cases here), which would attenuate unsteady effects (HX preheating). This work remains preliminary in terms of the study of fouling, and will require specific, more in-depth studies to gain a better understanding of fouling dynamics and purging techniques (mechanical, chemical and/or thermal).

CRediT authorship contribution statement

Jean-Baptiste Bouvenot: Writing – original draft, Visualization, Validation, Supervision, Resources, Project administration, Methodology, Investigation, Funding acquisition, Formal analysis, Data curation, Conceptualization. **Cyprien Beaudet:** Visualization, Formal analysis, Data curation.

Declaration of competing interest

The authors declare that they have no known competing financial interests or personal relationships that could have appeared to influence the work reported in this paper.

Acknowledgements

The authors would like to thank the Campus des métiers et des qualifications en éco-construction et en efficacité énergétique (CMQ3E) for their financial support.

Data availability

Data will be made available on request.

References

[1] Ministère de la transition écologique, Consommation d'énergie par usage du résidentiel, https://www.statistiques.developpement-durable.gouv.fr/consommation-denergie-par-usage-du-residentiel, le 22/05/2023 (consulkté le 10/10/2023).
[2] CEREN, «Données statistiques CEREN,» 2015.
[3] https://ec.europa.eu/eurostat/statistics explained/index.php?title=Energy_consumption_in_households.
[4] Department of Energy, https://www.energy.gov/energysaver/water-heating (consulté le 11/10/2023).
[5] E. Hervás-Blasco, E. Navarro-Peris, J.M. Corberán, Closing the residential energy loop: Grey-water heat recovery system for domestic hot water production based on heat pumps, Energ. Buildings 216 (2020) 109962, https://doi.org/10.1016/j.enbuild.2020.109962.
[6] SELIMLI, Selcuk et ELJETLAWI, M. Ibrahim Ali, The experimental study of thermal energy recovery from shower greywater, *Energy Sources Part A* 43 (23) (2021) 3032–3044.
[7] R. Vavřička, J. Boháč, T. Matuška, Experimental development of the plate shower heat exchanger to reduce the domestic hot water energy demand, Energ. Buildings 254 (2022) 111536, https://doi.org/10.1016/j.enbuild.2021.111536.
[8] Cooperman, Alissa et DIECKMANN, John, Drain water heat recovery, *ASHRAE J.* 53 (11) (2011) 58.
[9] Aonghus McNabola, Killian Shields, Efficient drain water heat recovery in horizontal domestic shower drains, Energy and Buildings, Volume 59, 2013, Pages 44-49, ISSN 0378-7788, doi: 10.1016/j.enbuild.2012.12.026. (https://www.sciencedirect.com/science/article/pii/S0378778812006755).
[10] S. Torras, C. Oliet, J. Rigola, A. Oliva, Drain water heat recovery storage-type unit for residential housing, Applied Thermal Engineering, Volume 103, 2016, Pages 670-683, ISSN 1359-4311, doi: 10.1016/j.applthermaleng.2016.04.086.
[11] L.T. Wong, K.W. Mui, Y. Guan, Shower water heat recovery in high-rise residential buildings of Hong Kong, Applied Energy, Volume 87, Issue 2, 2010, Pages 703-709, ISSN 0306-2619, doi: 10.1016/j.apenergy.2009.08.008.
[12] B. Scott, F. Ryan, F. Andrew, et al., Residential drain water heat recovery systems: Modeling, analysis, and implementation, *Journal of Green Building* 5 (3) (2010) 85–94.
[13] P. Jadwiszczak, E. Niemierka, Thermal effectiveness and NTU of horizontal plate drain water heat recovery unit - experimental study, *Int. Commun. Heat Mass Transfer* 147 (2023) 106938, https://doi.org/10.1016/j.icheatmasstransfer.2023.106938.
[14] Ramin Manouchehri, Carsen J. Banister, Michael R. Collins, Impact of small tilt angles on the performance of falling film drain water heat recovery systems,Energy and Buildings, Volume 102, 2015, Pages 181-186, ISSN 0378-7788, doi: 10.1016/j.enbuild.2015.05.024.
[15] Ivan Beentjes, Ramin Manouchehri, Michael R. Collins, An investigation of drain-side wetting on the performance of falling film drain water heat recovery systems, Energy and Buildings, Volume 82, 2014, Pages 660-667, ISSN 0378-7788, doi: 10.1016/j.enbuild.2014.07.069.
[16] Ramin Manouchehri, Michael R. Collins, An experimental analysis of the impact of unequal flow on falling film drain water heat recovery system performance, Energy and Buildings, Volume 165, 2018, Pages 150-159, ISSN 0378-7788, doi: 10.1016/j.enbuild.2018.01.018.
[17] Ramin Manouchehri, Michael R. Collins, An experimental analysis of the impact of temperature on falling film drain water heat recovery system effectiveness, Energy and Buildings, Volume 130, 2016, Pages 1-7, ISSN 0378-7788, doi: 10.1016/j.enbuild.2016.08.031.
[18] Manouchehri, R., and M. Collins. "Steady-state modelling of falling film drain water heat recovery performance using rated data." *eSim 2016 Building Performance Simulation Conference, May 3–6.* 2016.
[19] Zaloum, C., Lafrance, M., Gusdorf, J., n.d. Drain Water Heat Recovery Characterization and Modeling. https://builditsolar.com/Projects/WaterHeating/NRCanDrainWaterHtRecov.pdf.
[20] A.S. Dhillon An experimental approach towards characterizing the transient response of drain water heat recovery systems (Master's thesis 2019 University of Waterloo).

[21] Avis Technique n° 19/17-148_V1, 14 janvier 2021, CSTB https://www.cstb.fr/pdf/atec/GS19-T/AT17148_V1.pdf.
[22] Eslami-nejad, P., & Bernier, M. (2009). Impact of grey water heat recovery on the electrical demand of domestic hot water heaters https://www.aivc.org/sites/default/files/BS09_0681_687.pdf.
[23] D. Picard V. Delisle M. Bernier M. Kummert August). On the combined effect of wastewater heat recovery and solar domestic hot water heating In Canadian Solar Buildings Conference 2004.
[24] M. Salama, M.H. Sharqawy, Experimental investigation of the performance of a falling-film drain water heat recovery system, Appl. Therm. Eng. 179 (2020) 115712, https://doi.org/10.1016/j.applthermaleng.2020.115712.
[25] E. Ovadia, M.H. Sharqawy, Transient behavior of a falling-film drain water heat recovery device, thermal and economic performance assessments, Case Stud. Therm. Eng. 48 (2023) 103096, https://doi.org/10.1016/j.csite.2023.103096.
[26] E. Grundén M. Grischek Testing the Heat Transfer of a Drain Water Heat Recovery Heat Exchanger 2016 https://www.diva-portal.org/smash/get/diva2:952034/FULLTEXT01.pdf.
[27] O. Wanner, Biofilms, Les biofilms s'opposent à la récupération de chaleur Eawag News 60f/Juillet 2006, Eawag:, 2006, http://library.eawag.ch/eawag-publications/EAWAGnews/60F(2006).pdf.
[28] Chao Shen, Yiqiang Jiang, Yang Yao, Xinlei Wang, An experimental comparison of two heat exchangers used in wastewater source heat pump: A novel dry-expansion shell-and-tube evaporator versus a conventional immersed evaporator, Energy, Volume 47, Issue 1, 2012, Pages 600-608, ISSN 0360-5442, doi: 10.1016/j.energy.2012.09.043.
[29] Shen Chao, Jiang Yiqiang, Yao Yang, Deng Shiming, Experimental performance evaluation of a novel dry-expansion evaporator with defouling function in a wastewater source heat pump, Applied Energy, Volume 95, 2012, Pages 202-209, ISSN 0306-2619, doi: 10.1016/j.apenergy.2012.02.030.
[30] Chao Shen, Liangcheng Yang, Xinlei Wang, Yiqiang Jiang, Yang Yao, An experimental and numerical study of a de-fouling evaporator used in a wastewater source heat pump, Applied Thermal Engineering, Volume 70, Issue 1, 2014, Pages 501-509, ISSN 1359-4311, doi: 10.1016/j.applthermaleng.2014.05.055.
[31] Kiwa, -06 Nl "energieprestatie Van Gebouwen – Bepalingsmethode" (energy Performance of Buildings - Determination Method) NTA 8800 (2023) 2019.
[32] CSTB, Protocole RECADO, Mesurer la performance d'un système de récupération de chaleur sur les eaux de douches, CSTB, Mars 2015.
[33] CSA B55. 1-15 "Test method for measuring efficiency and pressure loss of drain water heat recovery units.".
[34] IAPMO IGC 347-2017 "Test method for measuring the performance of drain water heat recovery units.".
[35] B. Piotrowska, D. Słyś, Comprehensive Analysis of the State of Technology in the Field of Waste Heat Recovery from Grey Water, Energies 16 (1) (2023) 137, https://doi.org/10.3390/en16010137.
[36] Zahra Wehbi, Rani Taher, Jalal Faraj, Thierry Lemenand, Mehdi Mortazavi, Mahmoud Khaled, Waste Water Heat Recovery Systems types and applications: Comprehensive review, critical analysis, and potential recommendations, Energy Reports, Volume 9, Supplement 9, 2023, Pages 16-33, ISSN 2352-4847, doi: 10.1016/j.egyr.2023.05.243.
[37] Daniel Słyś, Sabina Kordana, Financial analysis of the implementation of a Drain Water Heat Recovery unit in residential housing, Energy and Buildings, Volume 71, 2014, Pages 1-11, ISSN 0378-7788, doi: 10.1016/j.enbuild.2013.11.088.
[38] Ehtech, OBOX-Récupérateur de chaleur sur eaux grises-Documentation technique, Août (2019). https://www.quantia.fr/wp-content/uploads/2021/06/Obox-Documentation-technique.pdf.
[39] L. Giraud, R. Baviere, M. Vallée, C. Paulus, September). Presentation, Validation and Application of the DistrictHeating Modelica Library Vol. 118 (2015) 79–88.
[40] AFNOR, NF EN 16147, Appareils pour eau chaude sanitaire, 2017.
[41] P. Kapustenko, J.J. Klemeš, O. Arsenyeva, Plate heat exchangers fouling mitigation effects in heating of water solutions: A review, Renew. Sustain. Energy Rev. 179 (2023) 113283.
[42] doi: 10.1016/j.rser.2023.113283Emilio Eguía, Alfredo Trueba, Belén Río-Calonge, Alfredo Girón, Carlos Bielva, Biofilm control in tubular heat exchangers refrigerated by seawater using flow inversion physical treatment, International Biodeterioration & Biodegradation, Volume 62, Issue 2, 2008, Pages 79-87, ISSN 0964-8305, doi: 10.1016/j.ibiod.2007.12.004.
[43] X. Zhiming, W. Jingtao, J. Yuting, et al., Experimental study on microbial fouling characteristics of the plate heat exchanger, *Appl. Therm. Eng.* 108 (2016) 150–157.
[44] C. Siyuan, C. Jinchun, S. Lin, Using thermal shock to inhibit biofilm formation in the treated sewage source heat pump systems, *Appl. Sci.* 7 (4) (2017) 343.
[45] C. Xiao, Y. Qirong, W. Ronghua, et al., Experimental study of the growth characteristics of microbial fouling on sewage heat exchanger surface, *Appl. Therm. Eng.* 128 (2018) 426–433.
[46] D. Kern, A theoretical analysis of thermal surface fouling, *Br. Chem. Eng.* 4 (1959) 258–262.
[47] A.R. Konak, Prediction of fouling curves in heat transfer equipment, *Trans. Inst. Chem. Eng* 51 (1973) 377.
[48] E. Nebot, J.F. Casanueva, T. Casanueva, et al., Model for fouling deposition on power plant steam condensers cooled with seawater: Effect of water velocity and tube material, *Int. J. Heat Mass Transf.* 50 (17–18) (2007) 3351–3358.
[49] T.A. Pogiatzis, V.S. Vassiliadis, F.J. Mergulhão, D.I. Wilson, Choosing When to Clean and How to Clean Biofilms in Heat Exchangers, Heat Transfer Eng. 36 (2015) 676–684, https://doi.org/10.1080/01457632.2015.954940.
[50] OLIVÈS, Régis et MANCAUX, Jean-Marie. Etude énergétique et environnementale des systèmes de production d'eau chaude sanitaire en France: lequel du chauffe-eau thermodynamique ou du chauffe-eau solaire est le plus soutenable?. In : *Congrès SFT*. Société Française de Thermique, 2024.